LETTER Communicated by Yann Le Cun

A Fast Learning Algorithm for Deep Belief Nets

Geoffrey E. Hinton
hinton@cs.toronto.edu
Simon Osindero
osindero@cs.toronto.edu
Department of Computer Science, University of Toronto, Toronto, Canada M5S 3G4

Yee-Whye Teh
tehyw@comp.nus.edu.sg
Department of Computer Science, National University of Singapore, Singapore 117543

We show how to use "complementary priors" to eliminate the explaining-away effects that make inference difficult in densely connected belief nets that have many hidden layers. Using complementary priors, we derive a fast, greedy algorithm that can learn deep, directed belief networks one layer at a time, provided the top two layers form an undirected associative memory. The fast, greedy algorithm is used to initialize a slower learning procedure that fine-tunes the weights using a contrastive version of the wake-sleep algorithm. After fine-tuning, a network with three hidden layers forms a very good generative model of the joint distribution of handwritten digit images and their labels. This generative model gives better digit classification than the best discriminative learning algorithms. The low-dimensional manifolds on which the digits lie are modeled by long ravines in the free-energy landscape of the top-level associative memory, and it is easy to explore these ravines by using the directed connections to display what the associative memory has in mind.

1 Introduction

Learning is difficult in densely connected, directed belief nets that have many hidden layers because it is difficult to infer the conditional distribution of the hidden activities when given a data vector. Variational methods use simple approximations to the true conditional distribution, but the approximations may be poor, especially at the deepest hidden layer, where the prior assumes independence. Also, variational learning still requires all of the parameters to be learned together and this makes the learning time scale poorly as the number of parameters increases.

We describe a model in which the top two hidden layers form an undirected associative memory (see Figure 1) and the remaining hidden layers so that the data flow refluxes

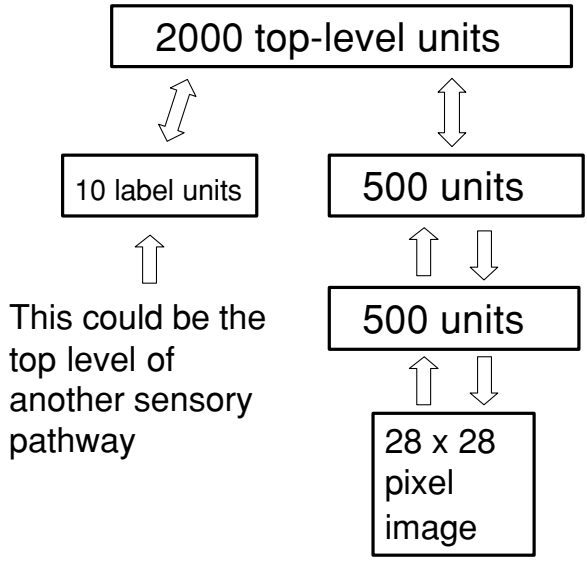

Figure 1: The network used to model the joint distribution of digit images and digit labels. In this letter, each training case consists of an image and an explicit class label, but work in progress has shown that the same learning algorithm can be used if the "labels" are replaced by a multilayer pathway whose inputs are spectrograms from multiple different speakers saying isolated digits. The network then learns to generate pairs that consist of an image and a spectrogram of the same digit class.

form a directed acyclic graph that converts the representations in the associative memory into observable variables such as the pixels of an image. This hybrid model has some attractive features:

- There is a fast, greedy learning algorithm that can find a fairly good set of parameters quickly, even in deep networks with millions of parameters and many hidden layers.
- The learning algorithm is unsupervised but can be applied to labeled data by learning a model that generates both the label and the data.
- There is a fine-tuning algorithm that learns an excellent generative model that outperforms discriminative methods on the MNIST database of hand-written digits.
- The generative model makes it easy to interpret the distributed representations in the deep hidden layers.

- The inference required for forming a percept is both fast and accurate.
- The learning algorithm is local. Adjustments to a synapse strength depend on only the states of the presynaptic and postsynaptic neuron.
- The communication is simple. Neurons need only to communicate their stochastic binary states.

Section 2 introduces the idea of a "complementary" prior that exactly cancels the "explaining away" phenomenon that makes inference difficult in directed models. An example of a directed belief network with complementary priors is presented. Section 3 shows the equivalence between restricted Boltzmann machines and infinite directed networks with tied weights.

Section 4 introduces a fast, greedy learning algorithm for constructing multilayer directed networks one layer at a time. Using a variational bound, it shows that as each new layer is added, the overall generative model improves. The greedy algorithm bears some resemblance to boosting in its repeated use of the same "weak" learner, but instead of reweighting each data vector to ensure that the next step learns something new, it re-represents it. The "weak" learner that is used to construct deep directed nets is itself an undirected graphical model.

Section 5 shows how the weights produced by the fast, greedy algorithm can be fine-tuned using the "up-down" algorithm. This is a contrastive version of the wake-sleep algorithm (Hinton, Dayan, Frey, & Neal, 1995) that does not suffer from the "mode-averaging" problems that can cause the wake-sleep algorithm to learn poor recognition weights.

Section 6 shows the pattern recognition performance of a network with three hidden layers and about 1.7 million weights on the MNIST set of handwritten digits. When no knowledge of geometry is provided and there is no special preprocessing, the generalization performance of the network is 1.25% errors on the 10,000-digit official test set. This beats the 1.5% achieved by the best backpropagation nets when they are not handcrafted for this particular application. It is also slightly better than the 1.4% errors reported by Decoste and Schoelkopf (2002) for support vector machines on the same task.

Finally, section 7 shows what happens in the mind of the network when it is running without being constrained by visual input. The network has a full generative model, so it is easy to look into its mind—we simply generate an image from its high-level representations.

Throughout the letter, we consider nets composed of stochastic binary variables, but the ideas can be generalized to other models in which the log probability of a variable is an additive function of the states of its directly connected neighbors (see appendix A for details).

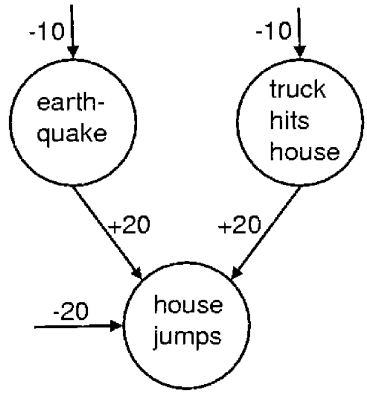

Figure 2: A simple logistic belief net containing two independent, rare causes that become highly anticorrelated when we observe the house jumping. The bias of -10 on the earthquake node means that in the absence of any observation, this node is e^{10} times more likely to be off than on. If the earthquake node is on and the truck node is off, the jump node has a total input of 0, which means that it has an even chance of being on. This is a much better explanation of the observation that the house jumped than the odds of e^{-20}, which apply if neither of the hidden causes is active. But it is wasteful to turn on both hidden causes to explain the observation because the probability of both happening is $e^{-10} \times e^{-10} = e^{-20}$. When the earthquake node is turned on, it "explains away" the evidence for the truck node.

2 Complementary Priors

The phenomenon of explaining away (illustrated in Figure 2) makes inference difficult in directed belief nets. In densely connected networks, the posterior distribution over the hidden variables is intractable except in a few special cases, such as mixture models or linear models with additive gaussian noise. Markov chain Monte Carlo methods (Neal, 1992) can be used to sample from the posterior, but they are typically very time-consuming. Variational methods (Neal & Hinton, 1998) approximate the true posterior with a more tractable distribution, and they can be used to improve a lower bound on the log probability of the training data. It is comforting that learning is guaranteed to improve a variational bound even when the inference of the hidden states is done incorrectly, but it would be much better to find a way of eliminating explaining away altogether, even in models whose hidden variables have highly correlated effects on the visible variables. It is widely assumed that this is impossible.

A logistic belief net (Neal, 1992) is composed of stochastic binary units. When the net is used to generate data, the probability of turning on unit i is a logistic function of the states of its immediate ancestors, j, and of the

weights, w_{ij}, on the directed connections from the ancestors:

$$p(s_i = 1) = \frac{1}{1 + \exp\left(-b_i - \sum_j s_j w_{ij}\right)}, \tag{2.1}$$

where b_i is the bias of unit i. If a logistic belief net has only one hidden layer, the prior distribution over the hidden variables is factorial because their binary states are chosen independently when the model is used to generate data. The nonindependence in the posterior distribution is created by the likelihood term coming from the data. Perhaps we could eliminate explaining away in the first hidden layer by using extra hidden layers to create a "complementary" prior that has exactly the opposite correlations to those in the likelihood term. Then, when the likelihood term is multiplied by the prior, we will get a posterior that is exactly factorial. It is not at all obvious that complementary priors exist, but Figure 3 shows a simple example of an infinite logistic belief net with tied weights in which the priors are complementary at every hidden layer (see appendix A for a more general treatment of the conditions under which complementary priors exist). The use of tied weights to construct complementary priors may seem like a mere trick for making directed models equivalent to undirected ones. As we shall see, however, it leads to a novel and very efficient learning algorithm that works by progressively untying the weights in each layer from the weights in higher layers.

2.1 An Infinite Directed Model with Tied Weights. We can generate data from the infinite directed net in Figure 3 by starting with a random configuration at an infinitely deep hidden layer[1] and then performing a top-down "ancestral" pass in which the binary state of each variable in a layer is chosen from the Bernoulli distribution determined by the top-down input coming from its active parents in the layer above. In this respect, it is just like any other directed acyclic belief net. Unlike other directed nets, however, we can sample from the true posterior distribution over all of the hidden layers by starting with a data vector on the visible units and then using the transposed weight matrices to infer the factorial distributions over each hidden layer in turn. At each hidden layer, we sample from the factorial posterior before computing the factorial posterior for the layer above.[2] Appendix A shows that this procedure gives unbiased samples

[1] The generation process converges to the stationary distribution of the Markov chain, so we need to start at a layer that is deep compared with the time it takes for the chain to reach equilibrium.

[2] This is exactly the same as the inference procedure used in the wake-sleep algorithm (Hinton et al., 1995) but for the models described in this letter no variational approximation is required because the inference procedure gives unbiased samples.

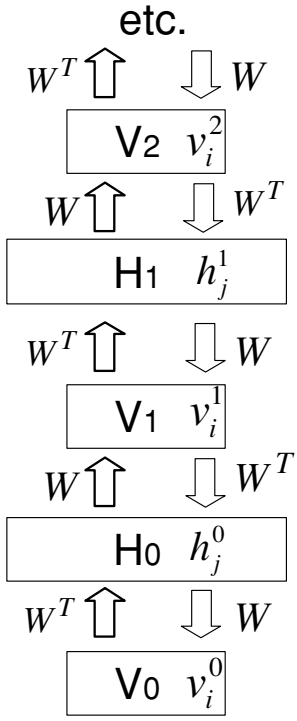

Figure 3: An infinite logistic belief net with tied weights. The downward arrows represent the generative model. The upward arrows are not part of the model. They represent the parameters that are used to infer samples from the posterior distribution at each hidden layer of the net when a data vector is clamped on V_0.

because the complementary prior at each layer ensures that the posterior distribution really is factorial.

Since we can sample from the true posterior, we can compute the derivatives of the log probability of the data. Let us start by computing the derivative for a generative weight, w_{ij}^{00}, from a unit j in layer H_0 to unit i in layer V_0 (see Figure 3). In a logistic belief net, the maximum likelihood learning rule for a single data vector, $\mathbf{v}^0$, is

It seems that p(v) is not defined by (2.1),
E = -sum(sum_{i ne j}(w_{ij} * h_j * v_i)/2
p(v) = 1/Z * exp(E(v))

$$\frac{\partial \log p(\mathbf{v}^0)}{\partial w_{ij}^{00}} = \langle h_j^0 (v_i^0 - \hat{v}_i^0) \rangle, \tag{2.2}$$

where $\langle \cdot \rangle$ denotes an average over the sampled states and $\hat{v}_i^0$ is the probability that unit i would be turned on if the visible vector was stochastically

reconstructed from the sampled hidden states. Computing the posterior distribution over the second hidden layer, V_1, from the sampled binary states in the first hidden layer, H_0, is exactly the same process as reconstructing the data, so v_i^1 is a sample from a Bernoulli random variable with probability $\hat{v}_i^0$. The learning rule can therefore be written as

$$\frac{\partial \log p(\mathbf{v}^0)}{\partial w_{ij}^{00}} = \langle h_j^0 (v_i^0 - v_i^1) \rangle. \tag{2.3}$$

The dependence of v_i^1 on h_j^0 is unproblematic in the derivation of equation 2.3 from equation 2.2 because $\hat{v}_i^0$ is an expectation that is conditional on h_j^0. Since the weights are replicated, the full derivative for a generative weight is obtained by summing the derivatives of the generative weights between all pairs of layers:

$$\frac{\partial \log p(\mathbf{v}^0)}{\partial w_{ij}} = \langle h_j^0 (v_i^0 - v_i^1) \rangle + \langle v_i^1 (h_j^0 - h_j^1) \rangle + \langle h_j^1 (v_i^1 - v_i^2) \rangle + \cdots \tag{2.4}$$

All of the pairwise products except the first and last cancel, leaving the Boltzmann machine learning rule of equation 3.1.

3 Restricted Boltzmann Machines and Contrastive Divergence Learning

It may not be immediately obvious that the infinite directed net in Figure 3 is equivalent to a restricted Boltzmann machine (RBM). An RBM has a single layer of hidden units that are not connected to each other and have undirected, symmetrical connections to a layer of visible units. To generate data from an RBM, we can start with a random state in one of the layers and then perform alternating Gibbs sampling. All of the units in one layer are updated in parallel given the current states of the units in the other layer, and this is repeated until the system is sampling from its equilibrium distribution. Notice that this is exactly the same process as generating data from the infinite belief net with tied weights. To perform maximum likelihood learning in an RBM, we can use the difference between two correlations. For each weight, w_{ij}, between a visible unit i and a hidden unit, j, we measure the correlation $\langle v_i^0 h_j^0 \rangle$ when a data vector is clamped on the visible units and the hidden states are sampled from their conditional distribution, which is factorial. Then, using alternating Gibbs sampling, we run the Markov chain shown in Figure 4 until it reaches its stationary distribution and measure the correlation $\langle v_i^\infty h_j^\infty \rangle$. The gradient of the log probability of the training data is then

$$\frac{\partial \log p(\mathbf{v}^0)}{\partial w_{ij}} = \langle v_i^0 h_j^0 \rangle - \langle v_i^\infty h_j^\infty \rangle. \tag{3.1}$$

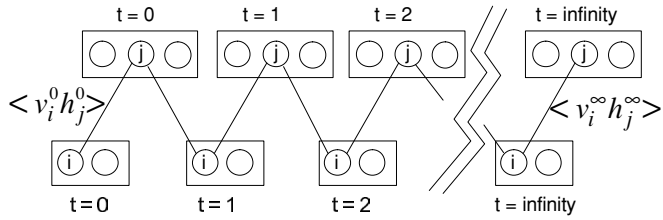

Figure 4: This depicts a Markov chain that uses alternating Gibbs sampling. In one full step of Gibbs sampling, the hidden units in the top layer are all updated in parallel by applying equation 2.1 to the inputs received from the the current states of the visible units in the bottom layer; then the visible units are all updated in parallel given the current hidden states. The chain is initialized by setting the binary states of the visible units to be the same as a data vector. The correlations in the activities of a visible and a hidden unit are measured after the first update of the hidden units and again at the end of the chain. The difference of these two correlations provides the learning signal for updating the weight on the connection.

This learning rule is the same as the maximum likelihood learning rule for the infinite logistic belief net with tied weights, and each step of Gibbs sampling corresponds to computing the exact posterior distribution in a layer of the infinite logistic belief net.

Maximizing the log probability of the data is exactly the same as minimizing the Kullback-Leibler divergence, $KL(P^0||P_\theta^\infty)$, between the distribution of the data, P^0, and the equilibrium distribution defined by the model, P_θ^∞. In contrastive divergence learning (Hinton, 2002), we run the Markov chain for only n full steps before measuring the second correlation.[3] This is equivalent to ignoring the derivatives that come from the higher layers of the infinite net. The sum of all these ignored derivatives is the derivative of the log probability of the posterior distribution in layer V_n, which is also the derivative of the Kullback-Leibler divergence between the posterior distribution in layer V_n, P_θ^n, and the equilibrium distribution defined by the model. So contrastive divergence learning minimizes the difference of two Kullback-Leibler divergences:

$$KL\left(P^0 \middle\| P_\theta^\infty\right) - KL\left(P_\theta^n \middle\| P_\theta^\infty\right). \tag{3.2}$$

Ignoring sampling noise, this difference is never negative because Gibbs sampling is used to produce P_θ^n from P^0, and Gibbs sampling always reduces the Kullback-Leibler divergence with the equilibrium distribution. It

[3] Each full step consists of updating **h** given **v**, then updating **v** given **h**.

is important to notice that P_θ^n depends on the current model parameters, and the way in which P_θ^n changes as the parameters change is being ignored by contrastive divergence learning. This problem does not arise with P^0 because the training data do not depend on the parameters. An empirical investigation of the relationship between the maximum likelihood and the contrastive divergence learning rules can be found in Carreira-Perpinan and Hinton (2005).

Contrastive divergence learning in a restricted Boltzmann machine is efficient enough to be practical (Mayraz & Hinton, 2001). Variations that use real-valued units and different sampling schemes are described in Teh, Welling, Osindero, and Hinton (2003) and have been quite successful for modeling the formation of topographic maps (Welling, Hinton, & Osindero, 2003) for denoising natural images (Roth & Black, 2005) or images of biological cells (Ning et al., 2005). Marks and Movellan (2001) describe a way of using contrastive divergence to perform factor analysis and Welling, Rosen-Zvi, and Hinton (2005) show that a network with logistic, binary visible units and linear, gaussian hidden units can be used for rapid document retrieval. However, it appears that the efficiency has been bought at a high price: When applied in the obvious way, contrastive divergence learning fails for deep, multilayer networks with different weights at each layer because these networks take far too long even to reach conditional equilibrium with a clamped data vector. We now show that the equivalence between RBMs and infinite directed nets with tied weights suggests an efficient learning algorithm for multilayer networks in which the weights are not tied.

4 A Greedy Learning Algorithm for Transforming Representations

How to train weights in this case?
how can we get the 'real' output of each model?

An efficient way to learn a complicated model is to combine a set of simpler models that are learned sequentially. To force each model in the sequence to learn something different from the previous models, the data are modified in some way after each model has been learned. In boosting (Freund, 1995), each model in the sequence is trained on reweighted data that emphasize the cases that the preceding models got wrong. In one version of principal components analysis, the variance in a modeled direction is removed, thus forcing the next modeled direction to lie in the orthogonal subspace (Sanger, 1989). In projection pursuit (Friedman & Stuetzle, 1981), the data are transformed by nonlinearly distorting one direction in the data space to remove all nongaussianity in that direction. The idea behind our greedy algorithm is to allow each model in the sequence to receive a different representation of the data. The model performs a nonlinear transformation on its input vectors and produces as output the vectors that will be used as input for the next model in the sequence.

Figure 5 shows a multilayer generative model in which the top two layers interact via undirected connections and all of the other connections

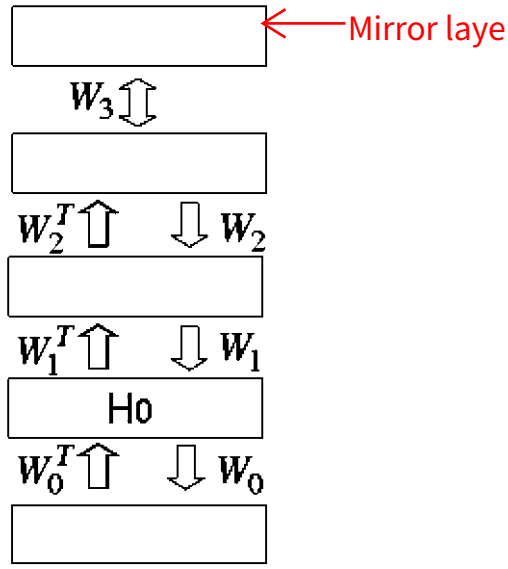

Figure 5: A hybrid network. The top two layers have undirected connections and form an associative memory. The layers below have directed, top-down generative connections that can be used to map a state of the associative memory to an image. There are also directed, bottom-up recognition connections that are used to infer a factorial representation in one layer from the binary activities in the layer below. In the greedy initial learning, the recognition connections are tied to the generative connections.

are directed. The undirected connections at the top are equivalent to having infinitely many higher layers with tied weights. There are no intralayer connections, and to simplify the analysis, all layers have the same number of units. It is possible to learn sensible (though not optimal) values for the parameters $\mathbf{W}_0$ by assuming that the parameters between higher layers will be used to construct a complementary prior for $\mathbf{W}_0$. This is equivalent to assuming that all of the weight matrices are constrained to be equal. The task of learning $\mathbf{W}_0$ under this assumption reduces to the task of learning an RBM, and although this is still difficult, good approximate solutions can be found rapidly by minimizing contrastive divergence. Once $\mathbf{W}_0$ has been learned, the data can be mapped through $\mathbf{W}_0^T$ to create higher-level "data" at the first hidden layer.

If the RBM is a perfect model of the original data, the higher-level "data" will already be modeled perfectly by the higher-level weight matrices. Generally, however, the RBM will not be able to model the original data perfectly, and we can make the generative model better using the following greedy algorithm:

1. Learn $\mathbf{W}_0$ assuming all the weight matrices are tied.
2. Freeze $\mathbf{W}_0$ and commit ourselves to using $\mathbf{W}_0^T$ to infer factorial approximate posterior distributions over the states of the variables in the first hidden layer, even if subsequent changes in higher-level weights mean that this inference method is no longer correct.
3. Keeping all the higher-weight matrices tied to each other, but untied from $\mathbf{W}_0$, learn an RBM model of the higher-level "data" that was produced by using $\mathbf{W}_0^T$ to transform the original data.

If this greedy algorithm changes the higher-level weight matrices, it is guaranteed to improve the generative model. As shown in Neal and Hinton (1998), the negative log probability of a single data vector, $\mathbf{v}^0$, under the multilayer generative model is bounded by a variational free energy, which is the expected energy under the approximating distribution, $Q(\mathbf{h}^0|\mathbf{v}^0)$, minus the entropy of that distribution. For a directed model, the "energy" of the configuration $\mathbf{v}^0, \mathbf{h}^0$ is given by

$$E(\mathbf{v}^0, \mathbf{h}^0) = -[\log p(\mathbf{h}^0) + \log p(\mathbf{v}^0|\mathbf{h}^0)], \tag{4.1}$$

so the bound is

$$\begin{aligned} \log p(\mathbf{v}^0) \geq & \sum_{\text{all } \mathbf{h}^0} Q(\mathbf{h}^0|\mathbf{v}^0)[\log p(\mathbf{h}^0) + \log p(\mathbf{v}^0|\mathbf{h}^0)] \\ & - \sum_{\text{all } \mathbf{h}^0} Q(\mathbf{h}^0|\mathbf{v}^0) \log Q(\mathbf{h}^0|\mathbf{v}^0), \end{aligned} \tag{4.2}$$

where $\mathbf{h}^0$ is a binary configuration of the units in the first hidden layer, $p(\mathbf{h}^0)$ is the prior probability of $\mathbf{h}^0$ under the current model (which is defined by the weights above H_0), and $Q(\cdot|\mathbf{v}^0)$ is any probability distribution over the binary configurations in the first hidden layer. The bound becomes an equality if and only if $Q(\cdot|\mathbf{v}^0)$ is the true posterior distribution.

When all of the weight matrices are tied together, the factorial distribution over H_0 produced by applying $\mathbf{W}_0^T$ to a data vector is the true posterior distribution, so at step 2 of the greedy algorithm, $\log p(\mathbf{v}^0)$ is equal to the bound. Step 2 freezes both $Q(\cdot|\mathbf{v}^0)$ and $p(\mathbf{v}^0|\mathbf{h}^0)$, and with these terms fixed, the derivative of the bound is the same as the derivative of

$$\sum_{\text{all } \mathbf{h}^0} Q(\mathbf{h}^0|\mathbf{v}^0) \log p(\mathbf{h}^0). \tag{4.3}$$

So maximizing the bound with respect to the weights in the higher layers is exactly equivalent to maximizing the log probability of a data set in which $\mathbf{h}^0$ occurs with probability $Q(\mathbf{h}^0|\mathbf{v}^0)$. If the bound becomes tighter, it

is possible for $\log p(\mathbf{v}^0)$ to fall even though the lower bound on it increases, but $\log p(\mathbf{v}^0)$ can never fall below its value at step 2 of the greedy algorithm because the bound is tight at this point and the bound always increases.

The greedy algorithm can clearly be applied recursively, so if we use the full maximum likelihood Boltzmann machine learning algorithm to learn each set of tied weights and then we untie the bottom layer of the set from the weights above, we can learn the weights one layer at a time with a guarantee that we will never decrease the bound on the log probability of the data under the model.[4] In practice, we replace the maximum likelihood Boltzmann machine learning algorithm by contrastive divergence learning because it works well and is much faster. The use of contrastive divergence voids the guarantee, but it is still reassuring to know that extra layers are guaranteed to improve imperfect models if we learn each layer with sufficient patience.

To guarantee that the generative model is improved by greedily learning more layers, it is convenient to consider models in which all layers are the same size so that the higher-level weights can be initialized to the values learned before they are untied from the weights in the layer below. The same greedy algorithm, however, can be applied even when the layers are different sizes.

5 Back-Fitting with the Up-Down Algorithm

Learning the weight matrices one layer at a time is efficient but not optimal. Once the weights in higher layers have been learned, neither the weights nor the simple inference procedure are optimal for the lower layers. The suboptimality produced by greedy learning is relatively innocuous for supervised methods like boosting. Labels are often scarce, and each label may provide only a few bits of constraint on the parameters, so overfitting is typically more of a problem than underfitting. Going back and refitting the earlier models may therefore cause more harm than good. Unsupervised methods, however, can use very large unlabeled data sets, and each case may be very high-dimensional, thus providing many bits of constraint on a generative model. Underfitting is then a serious problem, which can be alleviated by a subsequent stage of back-fitting in which the weights that were learned first are revised to fit in better with the weights that were learned later.

After greedily learning good initial values for the weights in every layer, we untie the "recognition" weights that are used for inference from the "generative" weights that define the model, but retain the restriction that the posterior in each layer must be approximated by a factorial distribution in which the variables within a layer are conditionally independent given

[4] The guarantee is on the expected change in the bound.

the values of the variables in the layer below. A variant of the wake-sleep algorithm described in Hinton et al. (1995) can then be used to allow the higher-level weights to influence the lower-level ones. In the "up-pass," the recognition weights are used in a bottom-up pass that stochastically picks a state for every hidden variable. The generative weights on the directed connections are then adjusted using the maximum likelihood learning rule in equation 2.2.[5] The weights on the undirected connections at the top level are learned as before by fitting the top-level RBM to the posterior distribution of the penultimate layer.

The "down-pass" starts with a state of the top-level associative memory and uses the top-down generative connections to stochastically activate each lower layer in turn. During the down-pass, the top-level undirected connections and the generative directed connections are not changed. Only the bottom-up recognition weights are modified. This is equivalent to the sleep phase of the wake-sleep algorithm if the associative memory is allowed to settle to its equilibrium distribution before initiating the down-pass. But if the associative memory is initialized by an up-pass and then only allowed to run for a few iterations of alternating Gibbs sampling before initiating the down-pass, this is a "contrastive" form of the wake-sleep algorithm that eliminates the need to sample from the equilibrium distribution of the associative memory. The contrastive form also fixes several other problems of the sleep phase. It ensures that the recognition weights are being learned for representations that resemble those used for real data, and it also helps to eliminate the problem of mode averaging. If, given a particular data vector, the current recognition weights always pick a particular mode at the level above and ignore other very different modes that are equally good at generating the data, the learning in the down-pass will not try to alter those recognition weights to recover any of the other modes as it would if the sleep phase used a pure ancestral pass. A pure ancestral pass would have to start by using prolonged Gibbs sampling to get an equilibrium sample from the top-level associative memory. By using a top-level associative memory, we also eliminate a problem in the wake phase: independent top-level units seem to be required to allow an ancestral pass, but they mean that the variational approximation is very poor for the top layer of weights.

Appendix B specifies the details of the up-down algorithm using MATLAB-style pseudocode for the network shown in Figure 1. For simplicity, there is no penalty on the weights, no momentum, and the same learning rate for all parameters. Also, the training data are reduced to a single case.

[5] Because weights are no longer tied to the weights above them, $\hat{v}_i^0$ must be computed using the states of the variables in the layer above i and the generative weights from these variables to i.

6 Performance on the MNIST Database

6.1 Training the Network. The MNIST database of handwritten digits contains 60,000 training images and 10,000 test images. Results for many different pattern recognition techniques are already published for this publicly available database, so it is ideal for evaluating new pattern recognition methods. For the basic version of the MNIST learning task, no knowledge of geometry is provided, and there is no special preprocessing or enhancement of the training set, so an unknown but fixed random permutation of the pixels would not affect the learning algorithm. For this "permutation-invariant" version of the task, the generalization performance of our network was 1.25% errors on the official test set. The network shown in Figure 1 was trained on 44,000 of the training images that were divided into 440 balanced mini-batches, each containing 10 examples of each digit class.[6] The weights were updated after each mini-batch.

In the initial phase of training, the greedy algorithm described in section 4 was used to train each layer of weights separately, starting at the bottom. Each layer was trained for 30 sweeps through the training set (called "epochs"). During training, the units in the "visible" layer of each RBM had real-valued activities between 0 and 1. These were the normalized pixel intensities when learning the bottom layer of weights. For training higher layers of weights, the real-valued activities of the visible units in the RBM were the activation probabilities of the hidden units in the lower-level RBM. The hidden layer of each RBM used stochastic binary values when that RBM was being trained. The greedy training took a few hours per layer in MATLAB on a 3 GHz Xeon processor, and when it was done, the error rate on the test set was 2.49% (see below for details of how the network is tested).

When training the top layer of weights (the ones in the associative memory), the labels were provided as part of the input. The labels were represented by turning on one unit in a "softmax" group of 10 units. When the activities in this group were reconstructed from the activities in the layer above, exactly one unit was allowed to be active, and the probability of picking unit i was given by

$$p_i = \frac{\exp(x_i)}{\sum_j \exp(x_j)}, \tag{6.1}$$

where x_i is the total input received by unit i. Curiously, the learning rules are unaffected by the competition between units in a softmax group, so the

[6] Preliminary experiments with 16×16 images of handwritten digits from the USPS database showed that a good way to model the joint distribution of digit images and their labels was to use an architecture of this type, but for 16×16 images, only three-fifths as many units were used in each hidden layer.

synapses do not need to know which unit is competing with which other unit. The competition affects the probability of a unit turning on, but it is only this probability that affects the learning.

After the greedy layer-by-layer training, the network was trained, with a different learning rate and weight decay, for 300 epochs using the up-down algorithm described in section 5. The learning rate, momentum, and weight decay[7] were chosen by training the network several times and observing its performance on a separate validation set of 10,000 images that were taken from the remainder of the full training set. For the first 100 epochs of the up-down algorithm, the up-pass was followed by three full iterations of alternating Gibbs sampling in the associative memory before performing the down-pass. For the second 100 epochs, 6 iterations were performed, and for the last 100 epochs, 10 iterations were performed. Each time the number of iterations of Gibbs sampling was raised, the error on the validation set decreased noticeably.

The network that performed best on the validation set was tested and had an error rate of 1.39%. This network was then trained on all 60,000 training images[8] until its error rate on the full training set was as low as its final error rate had been on the initial training set of 44,000 images. This took a further 59 epochs, making the total learning time about a week. The final network had an error rate of 1.25%.[9] The errors made by the network are shown in Figure 6. The 49 cases that the network gets correct but for which the second-best probability is within 0.3 of the best probability are shown in Figure 7.

The error rate of 1.25% compares very favorably with the error rates achieved by feedforward neural networks that have one or two hidden layers and are trained to optimize discrimination using the backpropagation algorithm (see Table 1). When the detailed connectivity of these networks is not handcrafted for this particular task, the best reported error rate for stochastic online learning with a separate squared error on each of the 10 output units is 2.95%. These error rates can be reduced to 1.53% in a net with one hidden layer of 800 units by using small initial weights, a separate cross-entropy error function on each output unit, and very gentle learning

[7] No attempt was made to use different learning rates or weight decays for different layers, and the learning rate and momentum were always set quite conservatively to avoid oscillations. It is highly likely that the learning speed could be considerably improved by a more careful choice of learning parameters, though it is possible that this would lead to worse solutions.

[8] The training set has unequal numbers of each class, so images were assigned randomly to each of the 600 mini-batches.

[9] To check that further learning would not have significantly improved the error rate, the network was then left running with a very small learning rate and with the test error being displayed after every epoch. After six weeks, the test error was fluctuating between 1.12% and 1.31% and was 1.18% for the epoch on which number of training errors was smallest.

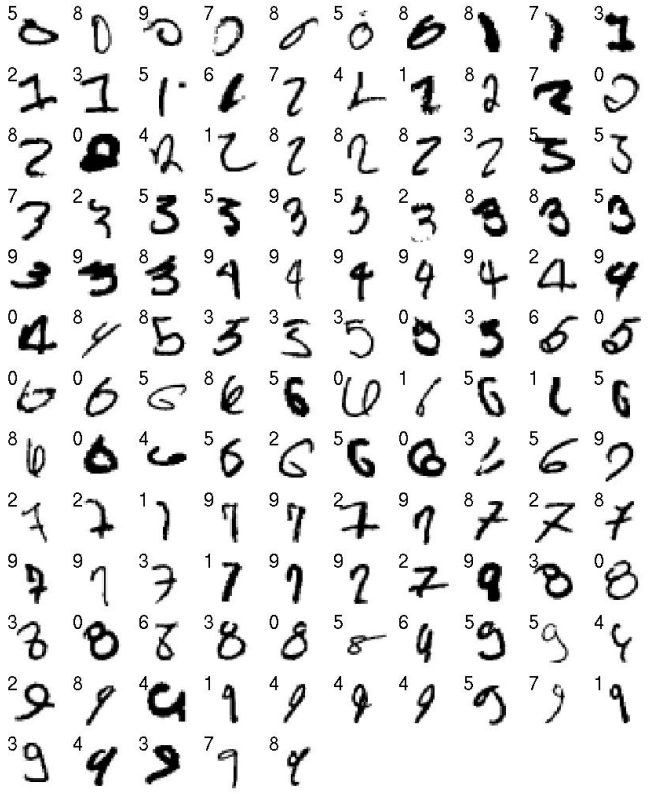

Figure 6: The 125 test cases that the network got wrong. Each case is labeled by the network's guess. The true classes are arranged in standard scan order.

(John Platt, personal communication, 2005). An almost identical result of 1.51% was achieved in a net that had 500 units in the first hidden layer and 300 in the second hidden layer by using "softmax" output units and a regularizer that penalizes the squared weights by an amount carefully chosen using a validation set. For comparison, nearest neighbor has a reported error rate (http://oldmill.uchicago.edu/wilder/Mnist/) of 3.1% if all 60,000 training cases are used (which is extremely slow) and 4.4% if 20,000 are used. This can be reduced to 2.8% and 4.0% by using an L3 norm.

The only standard machine learning technique that comes close to the 1.25% error rate of our generative model on the basic task is a support vector machine that gives an error rate of 1.4% (Decoste & Schoelkopf, 2002). But it is hard to see how support vector machines can make use of the domain-specific tricks, like weight sharing and subsampling, which LeCun, Bottou, and Haffner (1998) use to improve the performance of discriminative

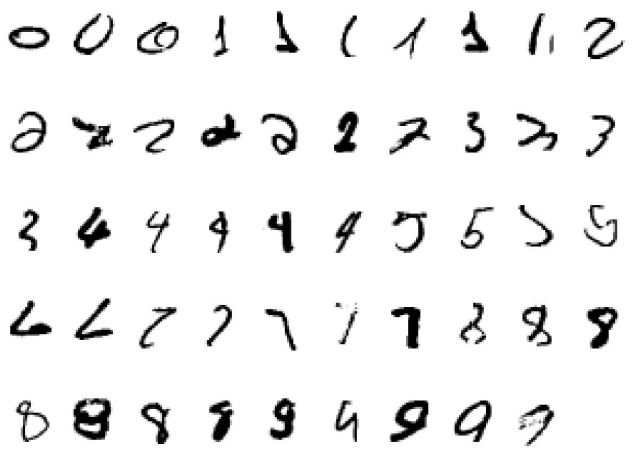

Figure 7: All 49 cases in which the network guessed right but had a second guess whose probability was within 0.3 of the probability of the best guess. The true classes are arranged in standard scan order.

neural networks from 1.5% to 0.95%. There is no obvious reason why weight sharing and subsampling cannot be used to reduce the error rate of the generative model, and we are currently investigating this approach. Further improvements can always be achieved by averaging the opinions of multiple networks, but this technique is available to all methods.

Substantial reductions in the error rate can be achieved by supplementing the data set with slightly transformed versions of the training data. Using one- and two-pixel translations, Decoste and Schoelkopf (2002) achieve 0.56%. Using local elastic deformations in a convolutional neural network, Simard, Steinkraus, and Platt (2003) achieve 0.4%, which is slightly better than the 0.63% achieved by the best hand-coded recognition algorithm (Belongie, Malik, & Puzicha, 2002). We have not yet explored the use of distorted data for learning generative models because many types of distortion need to be investigated, and the fine-tuning algorithm is currently too slow.

6.2 Testing the Network. One way to test the network is to use a stochastic up-pass from the image to fix the binary states of the 500 units in the lower layer of the associative memory. With these states fixed, the label units are given initial real-valued activities of 0.1, and a few iterations of alternating Gibbs sampling are then used to activate the correct label unit. This method of testing gives error rates that are almost 1% higher than the rates reported above.

Table 1: Error rates of Various Learning Algorithms on the MNIST Digit Recognition Task.

Version of MNIST Task	Learning Algorithm	Test Error %
Permutation invariant	Our generative model: $784 \rightarrow 500 \rightarrow 500 \leftrightarrow 2000 \leftrightarrow 10$	1.25
Permutation invariant	Support vector machine: degree 9 polynomial kernel	1.4
Permutation invariant	Backprop: $784 \rightarrow 500 \rightarrow 300 \rightarrow 10$ cross-entropy and weight-decay	1.51
Permutation invariant	Backprop: $784 \rightarrow 800 \rightarrow 10$ cross-entropy and early stopping	1.53
Permutation invariant	Backprop: $784 \rightarrow 500 \rightarrow 150 \rightarrow 10$ squared error and on-line updates	2.95
Permutation invariant	Nearest neighbor: all 60,000 examples and L3 norm	2.8
Permutation invariant	Nearest neighbor: all 60,000 examples and L2 norm	3.1
Permutation invariant	Nearest neighbor: 20,000 examples and L3 norm	4.0
Permutation invariant	Nearest neighbor: 20,000 examples and L2 norm	4.4
Unpermuted images; extra data from elastic deformations	Backprop: cross-entropy and early-stopping convolutional neural net	0.4
Unpermuted de-skewed images; extra data from 2 pixel translations	Virtual SVM: degree 9 polynomial kernel	0.56
Unpermuted images	Shape-context features: hand-coded matching	0.63
Unpermuted images; extra data from affine transformations	Backprop in LeNet5: convolutional neural net	0.8
Unpermuted images	Backprop in LeNet5: convolutional neural net	0.95

A better method is to first fix the binary states of the 500 units in the lower layer of the associative memory and to then turn on each of the label units in turn and compute the exact free energy of the resulting 510-component binary vector. Almost all the computation required is independent of which label unit is turned on (Teh & Hinton, 2001), and this method computes the exact conditional equilibrium distribution over labels instead of approximating it by Gibbs sampling, which is what the previous method is doing. This method gives error rates that are about 0.5% higher than the ones quoted because of the stochastic decisions made in the up-pass. We can remove this noise in two ways. The simpler is to make the up-pass deterministic by using probabilities of activation in place of

Figure 8: Each row shows 10 samples from the generative model with a particular label clamped on. The top-level associative memory is run for 1000 iterations of alternating Gibbs sampling between samples.

stochastic binary states. The second is to repeat the stochastic up-pass 20 times and average either the label probabilities or the label log probabilities over the 20 repetitions before picking the best one. The two types of average give almost identical results, and these results are also very similar to using a single deterministic up-pass, which was the method used for the reported results.

7 Looking into the Mind of a Neural Network

To generate samples from the model, we perform alternating Gibbs sampling in the top-level associative memory until the Markov chain converges to the equilibrium distribution. Then we use a sample from this distribution as input to the layers below and generate an image by a single down-pass through the generative connections. If we clamp the label units to a particular class during the Gibbs sampling, we can see images from the model's class-conditional distributions. Figure 8 shows a sequence of images for each class that were generated by allowing 1000 iterations of Gibbs sampling between samples.

We can also initialize the state of the top two layers by providing a random binary image as input. Figure 9 shows how the class-conditional state of the associative memory then evolves when it is allowed to run freely, but with the label clamped. This internal state is "observed" by performing a down-pass every 20 iterations to see what the associative memory has

Figure 9: Each row shows 10 samples from the generative model with a particular label clamped on. The top-level associative memory is initialized by an up-pass from a random binary image in which each pixel is on with a probability of 0.5. The first column shows the results of a down-pass from this initial high-level state. Subsequent columns are produced by 20 iterations of alternating Gibbs sampling in the associative memory.

in mind. This use of the word *mind* is not intended to be metaphorical. We believe that a mental state is the state of a hypothetical, external world in which a high-level internal representation would constitute veridical perception. That hypothetical world is what the figure shows.

8 Conclusion

We have shown that it is possible to learn a deep, densely connected belief network one layer at a time. The obvious way to do this is to assume that the higher layers do not exist when learning the lower layers, but this is not compatible with the use of simple factorial approximations to replace the intractable posterior distribution. For these approximations to work well, we need the true posterior to be as close to factorial as possible. So instead of ignoring the higher layers, we assume that they exist but have tied weights that are constrained to implement a complementary prior that makes the true posterior exactly factorial. This is equivalent to having an undirected model that can be learned efficiently using contrastive divergence. It can also be viewed as constrained variational learning because a penalty term—the divergence between the approximate and true

posteriors—has been replaced by the constraint that the prior must make the variational approximation exact.

After each layer has been learned, its weights are untied from the weights in higher layers. As these higher-level weights change, the priors for lower layers cease to be complementary, so the true posterior distributions in lower layers are no longer factorial, and the use of the transpose of the generative weights for inference is no longer correct. Nevertheless, we can use a variational bound to show that adapting the higher-level weights improves the overall generative model.

To demonstrate the power of our fast, greedy learning algorithm, we used it to initialize the weights for a much slower fine-tuning algorithm that learns an excellent generative model of digit images and their labels. It is not clear that this is the best way to use the fast, greedy algorithm. It might be better to omit the fine-tuning and use the speed of the greedy algorithm to learn an ensemble of larger, deeper networks or a much larger training set. The network in Figure 1 has about as many parameters as 0.002 cubic millimeters of mouse cortex (Horace Barlow, personal communication, 1999), and several hundred networks of this complexity could fit within a single voxel of a high-resolution fMRI scan. This suggests that much bigger networks may be required to compete with human shape recognition abilities.

Our current generative model is limited in many ways (Lee & Mumford, 2003). It is designed for images in which nonbinary values can be treated as probabilities (which is not the case for natural images); its use of top-down feedback during perception is limited to the associative memory in the top two layers; it does not have a systematic way of dealing with perceptual invariances; it assumes that segmentation has already been performed; and it does not learn to sequentially attend to the most informative parts of objects when discrimination is difficult. It does, however, illustrate some of the major advantages of generative models as compared to discriminative ones:

- Generative models can learn low-level features without requiring feedback from the label, and they can learn many more parameters than discriminative models without overfitting. In discriminative learning, each training case constrains the parameters only by as many bits of information as are required to specify the label. For a generative model, each training case constrains the parameters by the number of bits required to specify the input.
- It is easy to see what the network has learned by generating from its model.
- It is possible to interpret the nonlinear, distributed representations in the deep hidden layers by generating images from them.

- The superior classification performance of discriminative learning methods holds only for domains in which it is not possible to learn a good generative model. This set of domains is being eroded by Moore's law.

Appendix A: Complementary Priors

A.1 General Complementarity. Consider a joint distribution over observables, $\mathbf{x}$, and hidden variables, $\mathbf{y}$. For a given likelihood function, $P(\mathbf{x}|\mathbf{y})$, we define the corresponding family of complementary priors to be those distributions, $P(\mathbf{y})$, for which the joint distribution, $P(\mathbf{x}, \mathbf{y}) = P(\mathbf{x}|\mathbf{y})P(\mathbf{y})$, leads to posteriors, $P(\mathbf{y}|\mathbf{x})$, that exactly factorize, that is, leads to a posterior that can be expressed as $P(\mathbf{y}|\mathbf{x}) = \prod_j P(y_j|\mathbf{x})$.

Not all functional forms of likelihood admit a complementary prior. In this appendix, we show that the following family constitutes all likelihood functions admitting a complementary prior,

$$P(\mathbf{x}|\mathbf{y}) = \frac{1}{\Omega(\mathbf{y})} \exp\left(\sum_j \Phi_j(\mathbf{x}, y_j) + \beta(\mathbf{x})\right)$$

$$= \exp\left(\sum_j \Phi_j(\mathbf{x}, y_j) + \beta(\mathbf{x}) - \log \Omega(\mathbf{y})\right), \tag{A.1}$$

where Ω is the normalization term. For this assertion to hold, we need to assume positivity of distributions: that both $P(\mathbf{y}) > 0$ and $P(\mathbf{x}|\mathbf{y}) > 0$ for every value of $\mathbf{y}$ and $\mathbf{x}$. The corresponding family of complementary priors then assumes the form

$$P(\mathbf{y}) = \frac{1}{C} \exp\left(\log \Omega(\mathbf{y}) + \sum_j \alpha_j(y_j)\right), \tag{A.2}$$

where C is a constant to ensure normalization. This combination of functional forms leads to the following expression for the joint,

$$P(\mathbf{x}, \mathbf{y}) = \frac{1}{C} \exp\left(\sum_j \Phi_j(\mathbf{x}, y_j) + \beta(\mathbf{x}) + \sum_j \alpha_j(y_j)\right). \tag{A.3}$$

To prove our assertion, we need to show that every likelihood function of form equation A.1 admits a complementary prior and vice versa. First, it can be directly verified that equation A.2 is a complementary prior for the likelihood functions of equation A.1. To show the converse, let us assume that $P(\mathbf{y})$ is a complementary prior for some likelihood function $P(\mathbf{x}|\mathbf{y})$. Notice that the factorial form of the posterior simply means that the

joint distribution $P(\mathbf{x}, \mathbf{y}) = P(\mathbf{y})P(\mathbf{x}|\mathbf{y})$ satisfies the following set of conditional independencies: $y_j \perp\!\!\!\perp y_k \mid \mathbf{x}$ for every $j \neq k$. This set of conditional independencies corresponds exactly to the relations satisfied by an undirected graphical model having edges between every hidden and observed variable and among all observed variables. By the Hammersley-Clifford theorem and using our positivity assumption, the joint distribution must be of the form of equation A.3, and the forms for the likelihood function equation A.1 and prior equation A.2 follow from this.

A.2 Complementarity for Infinite Stacks. We now consider a subset of models of the form in equation A.3 for which the likelihood also factorizes. This means that we now have two sets of conditional independencies:

$$P(\mathbf{x}|\mathbf{y}) = \prod_i P(x_i|\mathbf{y}) \tag{A.4}$$

$$P(\mathbf{y}|\mathbf{x}) = \prod_j P(y_j|\mathbf{x}). \tag{A.5}$$

This condition is useful for our construction of the infinite stack of directed graphical models.

Identifying the conditional independencies in equations A.4 and A.5 as those satisfied by a complete bipartite undirected graphical model, and again using the Hammersley-Clifford theorem (assuming positivity), we see that the following form fully characterizes all joint distributions of interest,

$$P(\mathbf{x}, \mathbf{y}) = \frac{1}{Z} \exp\left(\sum_{i,j} \Psi_{i,j}(x_i, y_j) + \sum_i \gamma_i(x_i) + \sum_j \alpha_j(y_j) \right), \tag{A.6}$$

while the likelihood functions take on the form

$$P(\mathbf{x}|\mathbf{y}) = \exp\left(\sum_{i,j} \Psi_{i,j}(x_i, y_j) + \sum_i \gamma_i(x_i) - \log \Omega(\mathbf{y}) \right). \tag{A.7}$$

Although it is not immediately obvious, the marginal distribution over the observables, $\mathbf{x}$, in equation A.6 can also be expressed as an infinite directed model in which the parameters defining the conditional distributions between layers are tied together.

An intuitive way of validating this assertion is as follows. Consider one of the methods by which we might draw samples from the marginal distribution $P(\mathbf{x})$ implied by equation A.6. Starting from an arbitrary configuration of $\mathbf{y}$, we would iteratively perform Gibbs sampling using, in alternation, the distributions given in equations A.4 and A.5. If we run this Markov chain for long enough, then, under the mild assumption that the chain

mixes properly, we will eventually obtain unbiased samples from the joint distribution given in equation A.6.

Now let us imagine that we unroll this sequence of Gibbs updates in space, such that we consider each parallel update of the variables to constitute states of a separate layer in a graph. This unrolled sequence of states has a purely directed structure (with conditional distributions taking the form of equations A.4 and A.5 and in alternation). By equivalence to the Gibbs sampling scheme, after many layers in such an unrolled graph, adjacent pairs of layers will have a joint distribution as given in equation A.6.

We can formalize the above intuition for unrolling the graph as follows. The basic idea is to unroll the graph "upwards" (i.e., moving away from the data), so that we can put a well-defined distribution over the infinite stack of variables. Then we verify some simple marginal and conditional properties of the joint distribution and thus demonstrate the required properties of the graph in the "downwards" direction.

Let $\mathbf{x} = \mathbf{x}^{(0)}, \mathbf{y} = \mathbf{y}^{(0)}, \mathbf{x}^{(1)}, \mathbf{y}^{(1)}, \mathbf{x}^{(2)}, \mathbf{y}^{(2)}, \ldots$ be a sequence (stack) of variables, the first two of which are identified as our original observed and hidden variable. Define the functions

$$f(\mathbf{x}', \mathbf{y}') = \frac{1}{Z} \exp\left(\sum_{i,j} \Psi_{i,j}(x'_i, y'_i) + \sum_i \gamma_i(x'_i) + \sum_j \alpha_j(y'_j) \right) \tag{A.8}$$

$$f_x(\mathbf{x}') = \sum_{\mathbf{y}'} f(\mathbf{x}', \mathbf{y}') \tag{A.9}$$

$$f_y(\mathbf{y}') = \sum_{\mathbf{x}'} f(\mathbf{x}', \mathbf{y}') \tag{A.10}$$

$$g_x(\mathbf{x}'|\mathbf{y}') = f(\mathbf{x}', \mathbf{y}')/f_y(\mathbf{y}') \tag{A.11}$$

$$g_y(\mathbf{y}'|\mathbf{x}') = f(\mathbf{x}', \mathbf{y}')/f_x(\mathbf{x}'), \tag{A.12}$$

and define a joint distribution over our sequence of variables as follows:

$$P(\mathbf{x}^{(0)}, \mathbf{y}^{(0)}) = f\left(\mathbf{x}^{(0)}, \mathbf{y}^{(0)}\right) \tag{A.13}$$

$$P(\mathbf{x}^{(i)}|\mathbf{y}^{(i-1)}) = g_x\left(\mathbf{x}^{(i)}|\mathbf{y}^{(i-1)}\right) \qquad i = 1, 2, \ldots \tag{A.14}$$

$$P(\mathbf{y}^{(i)}|\mathbf{x}^{(i)}) = g_y\left(\mathbf{y}^{(i)}|\mathbf{x}^{(i)}\right). \qquad i = 1, 2, \ldots \tag{A.15}$$

We verify by induction that the distribution has the following marginal distributions:

$$P(\mathbf{x}^{(i)}) = f_x\left(\mathbf{x}^{(i)}\right) \qquad i = 0, 1, 2, \ldots \tag{A.16}$$

$$P(\mathbf{y}^{(i)}) = f_y\left(\mathbf{y}^{(i)}\right) \qquad i = 0, 1, 2, \ldots \tag{A.17}$$

For $i = 0$ this is given by definition of the distribution in equation A.13. For $i > 0$, we have:

$$P(\mathbf{x}^{(i)}) = \sum_{\mathbf{y}^{(i-1)}} P\left(\mathbf{x}^{(i)}|\mathbf{y}^{(i-1)}\right) P\left(\mathbf{y}^{(i-1)}\right) = \sum_{\mathbf{y}^{(i-1)}} \frac{f\left(\mathbf{x}^{(i)}, \mathbf{y}^{(i-1)}\right)}{f_y\left(\mathbf{y}^{(i-1)}\right)} f_y\left(\mathbf{y}^{(i-1)}\right)$$
$$= f_x\left(\mathbf{x}^{(i)}\right) \tag{A.18}$$

and similarly for $P(\mathbf{y}^{(i)})$. Now we see that the following conditional distributions also hold true:

$$P\left(\mathbf{x}^{(i)}|\mathbf{y}^{(i)}\right) = P\left(\mathbf{x}^{(i)}, \mathbf{y}^{(i)}\right) / P\left(\mathbf{y}^{(i)}\right) = g_x\left(\mathbf{x}^{(i)}|\mathbf{y}^{(i)}\right) \tag{A.19}$$

$$P\left(\mathbf{y}^{(i)}|\mathbf{x}^{(i+1)}\right) = P\left(\mathbf{y}^{(i)}, \mathbf{x}^{(i+1)}\right) / P\left(\mathbf{x}^{(i+1)}\right) = g_y\left(\mathbf{y}^{(i)}|\mathbf{x}^{(i+1)}\right). \tag{A.20}$$

So our joint distribution over the stack of variables also leads to the appropriate conditional distributions for the unrolled graph in the "downwards" direction. Inference in this infinite graph is equivalent to inference in the joint distribution over the sequence of variables, that is, given $\mathbf{x}^{(0)}$, we can obtain a sample from the posterior simply by sampling $\mathbf{y}^{(0)}|\mathbf{x}^{(0)}$, $\mathbf{x}^{(1)}|\mathbf{y}^{(0)}$, $\mathbf{y}^{(1)}|\mathbf{x}^{(1)}, \ldots$. This directly shows that our inference procedure is exact for the unrolled graph.

Appendix B: Pseudocode for Up-Down Algorithm

We now present MATLAB-style pseudocode for an implementation of the up-down algorithm described in section 5 and used for back-fitting. (This method is a contrastive version of the wake-sleep algorithm; Hinton et al., 1995.)

The code outlined below assumes a network of the type shown in Figure 1 with visible inputs, label nodes, and three layers of hidden units. Before applying the up-down algorithm, we would first perform layer-wise greedy training as described in sections 3 and 4.

```
\% UP-DOWN ALGORITHM
\%
\% the data and all biases are row vectors.
\% the generative model is: lab <--> top <--> pen --> hid --> vis
\% the number of units in layer foo is numfoo
\% weight matrices have names fromlayer_tolayer
\% "rec" is for recognition biases and "gen" is for generative
\% biases.
\% for simplicity, the same learning rate, r, is used everywhere.
```

```
\% PERFORM A BOTTOM-UP PASS TO GET WAKE/POSITIVE PHASE
\% PROBABILITIES AND SAMPLE STATES
wakehidprobs = logistic(data*vishid + hidrecbiases);
wakehidstates = wakehidprobs > rand(1, numhid);
wakepenprobs = logistic(wakehidstates*hidpen + penrecbiases);
wakepenstates = wakepenprobs > rand(1, numpen);
wakeopprobs = logistic(wakepenstates*pentop + targets*labtop +
  topbiases);
wakeopstates = wakeopprobs > rand(1, numtop);

\% POSITIVE PHASE STATISTICS FOR CONTRASTIVE DIVERGENCE
poslabtopstatistics = targets' * waketopstates;
pospentopstatistics = wakepenstates' * waketopstates;

\% PERFORM numCDiters GIBBS SAMPLING ITERATIONS USING THE TOP LEVEL
\% UNDIRECTED ASSOCIATIVE MEMORY
negtopstates = waketopstates; \% to initialize loop
for iter=1:numCDiters
  negpenprobs = logistic(negtopstates*pentop' + pengenbiases);
  negpenstates = negpenprobs > rand(1, numpen);
  neglabprobs = softmax(negtopstates*labtop' + labgenbiases);
  negtopprobs = logistic(negpenstates*pentop+neglabprobs*labtop+
    topbiases);
negtopstates = negtopprobs > rand(1, numtop));
end;
\% NEGATIVE PHASE STATISTICS FOR CONTRASTIVE DIVERGENCE
negpentopstatistics = negpenstates'*negtopstates;
neglabtopstatistics = neglabprobs'*negtopstates;

\% STARTING FROM THE END OF THE GIBBS SAMPLING RUN, PERFORM A
\% TOP-DOWN GENERATIVE PASS TO GET SLEEP/NEGATIVE PHASE
\% PROBABILITIES AND SAMPLE STATES
sleeppenstates = negpenstates;
sleephidprobs = logistic(sleeppenstates*penhid + hidgenbiases);
sleephidstates = sleephidprobs > rand(1, numhid);
sleepvisprobs = logistic(sleephidstates*hidvis + visgenbiases);

\% PREDICTIONS
psleeppenstates = logistic(sleephidstates*hidpen + penrecbiases);
psleephidstates = logistic(sleepvisprobs*vishid + hidrecbiases);
pvisprobs = logistic(wakehidstates*hidvis + visgenbiases);
phidprobs = logistic(wakepenstates*penhid + hidgenbiases);

\% UPDATES TO GENERATIVE PARAMETERS
hidvis = hidvis + r*poshidstates'*(data-pvisprobs);
```

```
visgenbiases = visgenbiases + r*(data - pvisprobs);
penhid = penhid + r*wakepenstates'*(wakehidstates-phidprobs);
hidgenbiases = hidgenbiases + r*(wakehidstates - phidprobs);

\% UPDATES TO TOP LEVEL ASSOCIATIVE MEMORY PARAMETERS
labtop = labtop + r*(poslabtopstatistics-neglabtopstatistics);
labgenbiases = labgenbiases + r*(targets - neglabprobs);
pentop = pentop + r*(pospentopstatistics - negpentopstatistics);
pengenbiases = pengenbiases + r*(wakepenstates - negpenstates);
topbiases = topbiases + r*(waketopstates - negtopstates);

\%UPDATES TO RECOGNITION/INFERENCE APPROXIMATION PARAMETERS
hidpen = hidpen + r*(sleephidstates'*(sleeppenstates-
  psleeppenstates));
penrecbiases = penrecbiases + r*(sleeppenstates-psleeppenstates);
vishid = vishid + r*(sleepvisprobs'*(sleephidstates-
  psleephidstates));
hidrecbiases = hidrecbiases + r*(sleephidstates-psleephidstates);
```

Acknowledgments

We thank Peter Dayan, Zoubin Ghahramani, Yann Le Cun, Andriy Mnih, Radford Neal, Terry Sejnowski, and Max Welling for helpful discussions and the referees for greatly improving the manuscript. The research was supported by NSERC, the Gatsby Charitable Foundation, CFI, and OIT. G.E.H. is a fellow of the Canadian Institute for Advanced Research and holds a Canada Research Chair in machine learning.

References

Belongie, S., Malik, J., & Puzicha, J. (2002). Shape matching and object recognition using shape contexts. *IEEE Transactions on Pattern Analysis and Machine Intelligence, 24*(4), 509–522.

Carreira-Perpinan, M. A., & Hinton, G. E. (2005). On contrastive divergence learning. In R. G. Cowell & Z. Ghahramani (Eds.), *Artificial Intelligence and Statistics, 2005*. (pp. 33–41). Fort Lauderdale, FL: Society for Artificial Intelligence and Statistics.

Decoste, D., & Schoelkopf, B. (2002). Training invariant support vector machines, *Machine Learning, 46*, 161–190.

Freund, Y. (1995). Boosting a weak learning algorithm by majority. *Information and Computation, 12*(2), 256–285.

Friedman, J., & Stuetzle, W. (1981). Projection pursuit regression. *Journal of the American Statistical Association, 76*, 817–823.

Hinton, G. E. (2002). Training products of experts by minimizing contrastive divergence, *Neural Computation, 14*(8), 1711–1800.

Hinton, G. E., Dayan, P., Frey, B. J., & Neal, R. (1995). The wake-sleep algorithm for self-organizing neural networks. *Science, 268*, 1158–1161.

LeCun, Y., Bottou, L., & Haffner, P. (1998). Gradient-based learning applied to document recognition. *Proceedings of the IEEE, 86*(11), 2278–2324.

Lee, T. S., & Mumford, D. (2003). Hierarchical Bayesian inference in the visual cortex. *Journal of the Optical Society of America, A, 20*, 1434–1448.

Marks, T. K., & Movellan, J. R. (2001). Diffusion networks, product of experts, and factor analysis. In T. W. Lee, T.-P. Jung, S. Makeig, & T. J. Sejnowski (Eds.), *Proc. Int. Conf. on Independent Component Analysis* (pp. 481–485). San Diego.

Mayraz, G., & Hinton, G. E. (2001). Recognizing hand-written digits using hierarchical products of experts. *IEEE Transactions on Pattern Analysis and Machine Intelligence, 24*, 189–197.

Neal, R. (1992). Connectionist learning of belief networks, *Artificial Intelligence, 56*, 71–113.

Neal, R. M., & Hinton, G. E. (1998). A new view of the EM algorithm that justifies incremental, sparse and other variants. In M. I. Jordan (Ed.), *Learning in graphical models* (pp. 355–368). Norwell, MA: Kluwer.

Ning, F., Delhomme, D., LeCun, Y., Piano, F., Bottou, L., & Barbano, P. (2005). Toward automatic phenotyping of developing embryos from videos. *IEEE Transactions on Image Processing, 14*(9), 1360–1371.

Roth, S., & Black, M. J. (2005). Fields of experts: A framework for learning image priors. In *IEEE Conf. on Computer Vision and Pattern Recognition* (pp. 860–867). Piscataway, NJ: IEEE.

Sanger, T. D. (1989). Optimal unsupervised learning in a single-layer linear feedforward neural networks. *Neural Networks, 2*(6), 459–473.

Simard, P. Y., Steinkraus, D., & Platt, J. (2003). Best practice for convolutional neural networks applied to visual document analysis. In *International Conference on Document Analysis and Recogntion (ICDAR)* (pp. 958–962). Los Alamitos, CA: IEEE Computer Society.

Teh, Y., & Hinton, G. E. (2001). Rate-coded restricted Boltzmann machines for face recognition. In T. K. Leen, T. G. Dietterich, & V. Tresp (Eds.), *Advances in neural information processing systems*, 13 (pp. 908–914). Cambridge, MA: MIT Press.

Teh, Y., Welling, M., Osindero, S., & Hinton, G. E. (2003). Energy-based models for sparse overcomplete representations. *Journal of Machine Learning Research, 4*, 1235–1260.

Welling, M., Hinton, G., & Osindero, S. (2003). Learning sparse topographic representations with products of Student-t distributions. In S. Becker, S. Thrun, & K. Obermayer (Eds.), *Advances in neural information processing systems, 15* (pp. 1359–1366). Cambridge, MA: MIT Press.

Welling, M., Rosen-Zvi, M., & Hinton, G. E. (2005). Exponential family harmoniums with an application to information retrieval. In L. K. Saul, Y. Weiss, & L. Bottou (Eds.), *Advances in neural information processing systems, 17* (pp. 1481–1488). Cambridge, MA: MIT Press.

Received June 8, 2005; accepted November 8, 2005.